



A simple generative model of trilobite segmentation and growth

RESEARCH ARTICLE

Melanie J Hopkins¹

¹ Division of Paleontology (Invertebrates), American Museum of Natural History – New York, USA

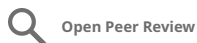
Cite as: Hopkins MJ (2020). A simple generative model of trilobite segmentation and growth. *PaleoXiv* version 3, peer-reviewed by PCI Paleo. doi: 10.31233/osf.io/zt642

Published: 27 January 2020

Recommender:
Christian Klug

Reviewers:
Kenneth De Baets and Lukáš Laibl

Correspondence:
mhopkins@amnh.org



© 2020 Author(s)



This work is licensed under the Creative Commons Attribution 4.0 International License.

THIS ARTICLE HAS BEEN PEER-REVIEWED BY PCI PALEO

Read the Editor's recommendation and Referees' reports at [DOI:10.24072/pci.paleo.100004](https://doi.org/10.24072/pci.paleo.100004)

ABSTRACT

Generative growth models have been the basis for numerous studies of morphological diversity and evolution. Most work has focused on modeling accretionary growth systems, with much less attention to discrete growth systems. Generative growth models for molting organisms, such as arthropods, have remained particularly elusive. However, our understanding of post-embryonic growth in trilobite species is sufficiently mature that it is now possible to model growth in a way that incorporates the addition of new parts as well as differential growth rates for existing parts across the trilobite body plan. Furthermore, body size data for a large sample of specimens of the trilobite species *Aulacopleura koninckii* (Barrande, 1846) make it possible to generate robust estimates for model parameters. Although the generative model described here was based on a relatively simple segmentation schedule, a diverse array of observed body sizes and relative proportions of body regions can be attained by altering only a few parameters at a time. Notably, small changes in growth rates can have large effects on body size (e.g. an increase of 4% increases body size by 350%). Subsampling of the empirical dataset indicates that parameters describing the growth gradient in the trunk are more sensitive to sample size than input parameters. Increasing the number of stages represented improves parameter estimates more quickly than increasing number of specimens per stage.

Keywords: trilobites; theoretical morphology; growth model; growth rates; development

Introduction

Generative growth models have long attracted biologists and mathematicians. Some of the earliest work focused on the geometric form of coiled invertebrates, such as gastropods (e.g., [Thompson, 1942](#)). In particular, the work by David Raup ([1961; 1966](#)) was foundational for subsequent studies of mollusk growth and morphology using model-based descriptors, and as a result, mollusks have become a model group for studying accretionary growth, and theoretical modeling of morphology more generally ([Urdy et al., 2010; Urdy, 2015](#)). Although generative models for other types of organisms have also been proposed (see [McGhee, 1999, 2015](#) for examples), arthropods have remained elusive, as “discrete growth systems are more difficult to model than accretionary growth systems. Perhaps the ultimate nightmare of any modeler of morphogenesis is organisms that molt, whose entire skeleton is episodically shed and regrown, often with the new skeleton possessing parts or elements not previously present in the organism” ([McGhee, 1999, p. 142](#)).

Trilobites are an extinct group of marine arthropods with one of the best fossil records of any arthropod group. In part, this is due to the fact that the trilobite dorsal exoskeleton was highly impregnated with low-magnesium calcite ([Wilmot and Fallick, 1989](#)). Because trilobites started biomineralizing the exoskeleton at very early post-embryonic stages, the growth and morphological development of many species can be pieced together from samples that include fossilized exuviae as well as individual body fossils ([Hopkins, 2017](#)). With enough well-preserved specimens, it is possible to chart segmentation patterns and estimate growth rates. Segmentation and growth patterns in trilobites are now sufficiently well understood (e.g., [Hughes, 2003a,b; Minelli et al., 2003; Hughes, 2005; Hughes et al., 2006; Hughes, 2007; Minelli and Fusco, 2013; Fusco et al., 2014; Hong et al., 2014; Fusco et al., 2016](#)) that generative growth models are within reach. Further, measurements of body size and body proportions for a large sample of specimens are now available for one of the best studied trilobite species in this regard, *Aulacopleura koninckii* ([Barrande, 1846](#)) ([Hughes et al., 2017](#)). In this paper, I use these studies as a basis for developing a simple generative model for trilobites and explore the impact of varying different parameters on body size and body proportions.

Segmentation patterns and growth during trilobite ontogeny

Like some centipedes and most crustaceans, the final segmental composition of the trilobite body was attained during post-embryonic ontogeny through a series of molts ([Fusco and Minelli, 2013](#)). Trilobites had a hemianamorphic mode of segmentation, meaning they underwent a phase of molts during which new segments were added to the body followed by a phase during which molting continued without further increase in the number of body segments ([Minelli et al., 2003; Minelli and Fusco, 2013](#)). In trilobites, the earliest biomineralized molt was a single articulated sclerite comprised of some number of fused segments; this has been termed the protaspid period. The subsequent meraspid period began when molting resulted in the first articulation between the cephalon and the transitory pygidium, each comprised of fused segments. During subsequent molts, either new segments were generated near the posterior end of the transitory pygidium, or a new articulation appeared at the anterior end of the transitory pygidium (i.e., a thoracic tergite¹ was released into the thorax), or both. At some point, segment generation ceased (ending the anamorphic phase and initiating the epimorphic phase) and articulation

¹Traditionally, the articulated sclerites in the thorax of the trilobite exoskeleton have been called “thoracic segments”. Throughout this manuscript, I refer to the thoracic segments as “tergites” to reflect their anatomical similarity to other arthropods and distinguish them from body segments, which may not be positionally synchronous ([Ortega-Hernández and Brena, 2012](#)).

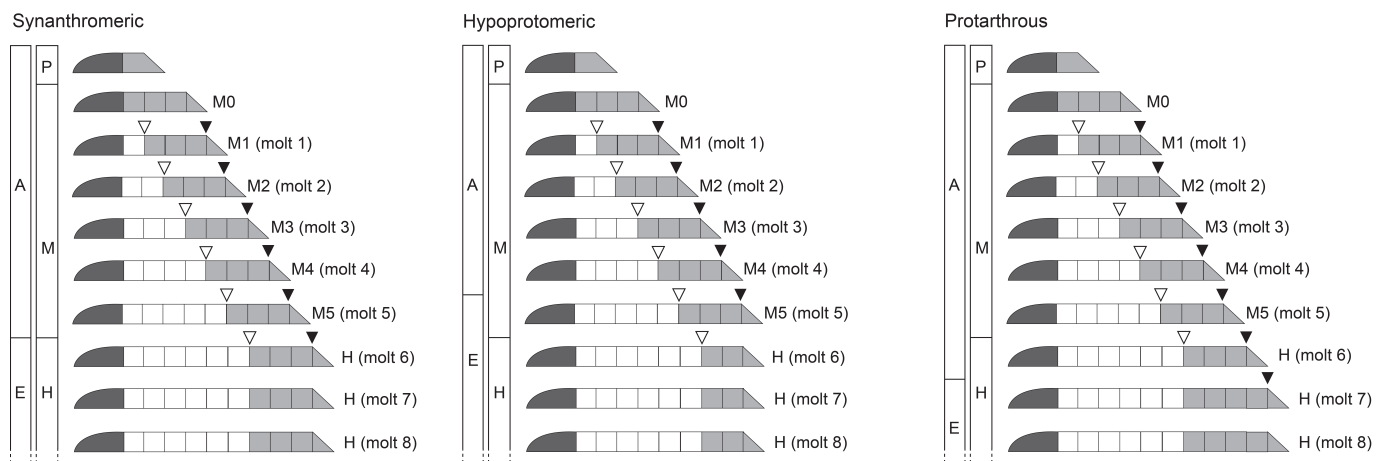


Figure 1. Schematics showing hemianamorphic mode of segmentation in trilobites. Trilobites underwent a phase of molts during which new segments were added to the body (anamorphosis, “A”) followed by a phase of molts during which molting continued without further increase in the number of body segments (epimorphosis, “E”); the addition of a new segment is marked with a black triangle at the point of insertion. Trilobites also underwent a phase of molts during which new articulations between exoskeletal sclerites were added to the body (meraspis, “M”) followed by a phase of molts during which molting continued without further increase in number of articulations (holaspis, “H”); the addition of a new articulation is marked with a white triangle at the point of insertion. It is customary to refer to the meraspid molt stages by the prefix “M” followed by the number of thoracic tergites in the body. The relative timing of these transitions could vary; three schedules (synanthromeric, hypoprotomeric, and protarthrous) observed in trilobites are shown (see text for more detail). In these examples, the trilobite entered the holaspid period at molt 6, at which point the body was composed of a cephalon (dark gray), six thoracic tergites (white squares), and a pygidium with either two or three fused segments (light gray squares) plus a terminal piece (triangle). The cephalon, each thoracic tergite, and the pygidium are articulated. Graphical form based on schematics introduced by Hughes et al. (2006).

generation ceased (ending the meraspid period and initiating the holaspid period) (Fig. 1). The relative timing of these transitions varied across species, and three different schedules have been documented in trilobites: 1) hypoprotomeric, where individuals entered the epimorphic phase within the meraspid period (the cessation of new segment generation preceded the cessation of new thoracic articulation); 2) synanthromeric, where individuals entered the epimorphic phase and holaspid period synchronously; and 3) protarthrous, where individuals entered the epimorphic phases within the holaspid period (the cessation of new thoracic articulation preceded the cessation of new segment generation in the pygidium) (Fig. 1; Hughes et al., 2006).

During the meraspid period, the number of tergites in the thorax is a size-independent measure of relative age of the individuals. Per-molt size increase was constant for some sclerites for some portions of the ontogeny in at least some trilobites (Chatterton et al., 1990; Fusco et al., 2012), but detailed data-rich studies of the trilobite *Aulocopleura koninckii* indicate that the rate of growth in the thorax was governed by a growth field described by a continuous gradient rather than constant per-tergite rates (Fusco et al., 2014, 2016).

Description of the growth model

Because total body size at any given point during ontogeny (as well as potential maximum body size) was determined both by the segmentation schedule and the pattern of growth rates, several parameters are needed in order to model trilobite growth. Parameters are summarized in Table 1 and Figure 2. An R function for running the growth model using these parameters is available at www.github.com/melj/trilobite-growth.

Table 1. Parameters (all single variables) that can be adjusted in the model and parameter estimates for *Aulacopleura koninckii* (based on data from Hughes et al., 2017). An R function for calculating these estimates from the dataset is available at www.github.com/melj/trilo-growth.

Parameter	Description	Parameter estimates for <i>A. koninckii</i>
<i>Molt</i>	Number of molts in lifespan, and the number of time steps in the model	31
<i>Ter</i>	Number of molts during meraspid period	20
<i>ce</i>	Length of the cephalon at M0	0.671
<i>p</i>	Length of transitory pygidium at M0	0.549
<i>t.p</i>	Length of newly released tergite, as proportion of pygidial length in previous stage	0.182
<i>R</i>	Stage at which rates transition from “initial/meraspid growth gradient” to “final/holaspid growth gradient”	20
<i>lowM</i>	Minimum growth rate (of growth gradient) for thorax during meraspis ($\pm R$); equivalent to a in exponential decay function	1.060
<i>highM</i>	Maximum growth rate (of growth gradient) for thorax during meraspis ($\pm R$); equivalent to $a + b$ in exponential decay function	1.370
<i>lambdaM</i>	Exponential decay constant defining growth gradient during meraspis ($\pm R$); equivalent to λ in exponential decay function	5.001
<i>lowH</i>	Minimum growth rate (of growth gradient) for thorax during holaspis (or post- R); equivalent to a in exponential decay function	1.084
<i>highH</i>	Maximum growth rate (of growth gradient) for thorax during holaspis (or post- R); equivalent to $a + b$ in exponential decay function	1.168
<i>lambdaH</i>	Exponential decay constant defining growth gradient during holaspis (or post- R); equivalent to λ in exponential decay function	5.806
<i>g.c</i>	Growth rate of cephalon, assumed constant throughout lifespan	1.085

Cephalic growth

Growth rate of cephalon (*g.c*)

Although the relative size of features on the cephalon (e.g., the length of the glabella relative to the length of the cephalon) changed during ontogeny (Fusco et al., 2016; Hopkins and Pearson, 2016; Hopkins, 2017), this model assumes that the growth rate of the cephalon as a whole was constant (Chatterton et al., 1990; Fusco et al., 2012). For each molt M , the size of the cephalon is estimated as $ce * g.c^M$ where ce is the initial size of the cephalon at M0 (see below) and $g.c$ is the growth rate.

Defining the growth gradient of the trunk

Fusco et al. (2014) found that an exponential decay function best described the distribution of per-molt local growth rates across the trunk during the meraspid period, specifically that the growth at relative position x along the trunk = $a + b * exp(-\lambda(1 - x))$. When $x = 0$, this equation simplifies to growth rate = a ; this is the lower bound for the growth gradient (*lowM* in Table 1 and Figure 2). When $x = 1$, the equation simplifies to growth = $a + b$; this sum is the upper bound for the growth gradient (*highM* in Table 1 and Figure 2). The exponential decay constant (λ) describes the concavity of the exponential decay curve, and is represented in the model by the parameter *lambdaM* (Table 1 and Figure 2). Because the growth gradient may shift during the transition from the meraspid to holaspid stages (Fusco et al., 2016), three additional parameters are included to describe the holaspid growth gradient (*lowH*, *highH*, and *lambdaH* in Table 1 and Figure 2).

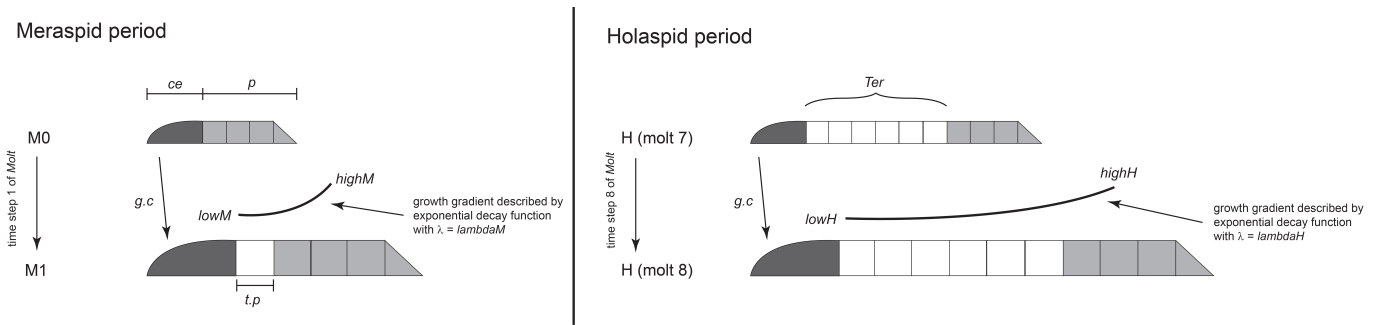


Figure 2. Schematic showing model parameters during the meraspid and holaspid periods. Dark gray = cephalon; white = thorax comprised of articulated sclerites; light gray = pygidium comprised of fused segments. Not shown is the parameter R which determines the timing of the transition from the meraspid growth gradient to the holaspid growth gradient. See text and Table 1 for more detail.

This gradient includes the pygidium, but newly released tergites were sourced from the anterior region of the growing transitory pygidium. Therefore the model effectively takes the following steps to determine the lengths of the tergites and transitory pygidium in each subsequent molt during the meraspid period:

1. Determine the relative position along the trunk of the median points of each tergite and on the transitory pygidium at the preceding molt.
2. Sample the exponential decay function at these relative positions to generate a vector of growth rates along the trunk.
3. Apply these rates to the respective lengths of each tergite and the transitory pygidium.

At this point the new length of the “pygidium” is the sum of the length of the new transitory pygidium and the length of the newly released tergite. Therefore the following additional steps are required:

4. Assign a length to the newly released tergite (see below).
5. Determine the length of the new transitory pygidium by subtracting the length of the newly released tergite.

For the holaspid period, the model follows steps 1–3 for each molt.

Parameters determining initial input and transition points

Number of molts in lifespan ($Molt$)

The number of molts determines the number of time-steps in the model. The only restriction on this parameter is that it must be greater than the number of molts during the meraspid period (Ter). The specimen modeled at $Molt = 0$ is conveniently the M0 stage (see Figure 1).

Number of molts during meraspid period (Ter)

For most trilobite species, a thoracic tergite was released at each molt during the meraspid period. Thus this parameter will be equal to the terminal number of thoracic tergites for most species. The model currently does not accommodate exceptions (such as molts accompanied by no tergite release or multiple tergite release), although this could be modified in the future. In the model, when $Molt < Ter$, the parameters describing the growth gradient change are those defined for the meraspid period; when $Molt \geq Ter$, the parameters describing the growth gradient are those defined for the holaspid period (see above).

Length of cephalon and transitory pygidium at M0 (ce and p , respectively)

These parameters describe the size of the trilobite at the onset of epimorphic growth, where M0 refers to the molt characterized by one articulation between the cephalon and the transitory pygidium (Figs 1, 2). These parameters set the initial size of the trilobite and can be estimated directly from fossil specimens or estimated from growth series.

Length of newly released tergite ($t.p$)

This parameter determines the size of the tergite released from the transitory pygidium at each molt during meraspis (Fig. 2). Because the new tergite was sourced from the anterior region of the pygidium, the length of the newly-released tergite may be defined as a proportion of the pygidial length after the growth gradient has been applied.

Number of molts during which initial or “meraspid” growth gradient is active (R)

It is possible that the growth gradient did not always change at the start of holaspis. This parameter defines the number of molts for which the initial growth gradient was still active. It is thus constrained to range from zero to $Molt$. If $R < Ter$, then the change in growth rates occurs before the last tergite is released into the thorax. If $R > Ter$, then the change in growth rates occurs after the last tergite is released. If $R = Ter$, then the transition occurs at the same time as the last tergite is released. If $R = Molt$, then there is no transition to a new growth gradient.

If the transition to the holaspid growth gradient coincided with the onset of epimorphosis, then the different segmentation schedules (Fig. 1) could be implemented by varying this parameter appropriately. However, this is a hypothesis that has yet to be tested. It is also possible that the growth gradient changed gradually throughout ontogeny in some trilobites. This is not accommodated in the current model but could be potentially accommodated in the future by defining vectors of molt-dependent growth rates.

Parameter estimates from empirical data

I used a data set of measurements from *Aulacopleura koninckii* specimens (Hughes et al., 2017) to estimate values for each model parameter. A representative holaspid specimen of *A. koninckii* is shown in Supplementary Figure S1A; for additional specimens, including meraspid stages, see Hong et al. (2014).

Cephalic growth rate ($g.c$)

The cephalic growth rate was estimated using the slope of the OLS regression of logged cephalic lengths against the number of tergites in the thorax for all specimens certain to be meraspids². For *Aulacopleura koninckii*, lines were fit to juvenile stages 9-17 ($N = 137$) because the number of specimens representing earlier stages were too few ($N = 11$), following Fusco et al. (2014) (Fig. 1A). Including the earliest stages slightly alters the parameter estimates and the model output (Fig. S2).

Meraspid growth gradient

The number of tergites provides a size-independent measurement of age during the meraspid stage. For meraspids, model parameters a , b , and λ were estimated by fitting an exponential curve to average

²*Aulacopleura koninckii* had a variable terminal number of thoracic tergites, ranging from 18 to 22 (see section Holaspid growth gradient for further discussion). Therefore only specimens with 17 or fewer tergites are certain to be meraspids.

per-molt tergite growth rates against relative tergite position in the trunk. The relative position in the trunk of the posterior margin of each tergite was calculated by scaling the cumulative average lengths of the trunk sclerites to range from 0 to 1 and then finding the midpoint of each tergite along this range. Growth rates between stages were calculated by dividing the average tergite lengths in stage $i + 1$ by the averages in stage i . For *Aulacopleura koninckii*, curves were fit to juvenile stages 9–17 ($N = 137$) because the number of specimens representing earlier stages were too few ($N = 11$), following Fusco et al. (2014). Including the earliest stages slightly alters the parameter estimates and the model output (Fig. S2).

Holaspid growth gradient

Unlike meraspids, holaspids are characterized by having the same number of tergites, so this trait cannot be used as a size-independent measure of age. However, because cephalic growth rates are assumed to be constant across ontogeny, holaspids can be assigned to molt stages by extrapolating from an OLS regression of $\ln(\text{cephalic length})$ against molt stage from meraspid specimens (Fusco et al., 2016). Model parameters a , b , and λ are then estimated in the same fashion as for the meraspid growth gradient. *Aulacopleura koninckii* has a variable terminal number of tergites, ranging from 18 to 22 and yielding 5 holaspid morphotypes. Note that *A. koninckii* provides an unusual case study for trilobites in having had a variable terminal number of thoracic tergites. For most species there appears to be no variation, and in some clades the terminal number of tergites was highly conserved (e.g., Lichidae species had 11 tergites at the onset of epimorphosis; Thomas and Holloway, 1988; Whittington, 2002).

Fusco et al. (2016) found that growth gradients were similar among holaspid morphotypes; for this study, parameters were estimated using specimens with 20 tergites because this is the median terminal number of thoracic tergites achieved by *A. koninckii* individuals. Growth gradient curves are shown in Figure 3B.

Number of molts in lifespan ($Molt$)

The total number of molts was set to the maximum estimated holaspid stage (see Holaspid growth gradient above).

Number of molts during meraspid period (Ter)

The total number of molts during the meraspid stage was set to 20 for *Aulacopleura koninckii*, which is the median terminal number of thoracic tergites achieved by *A. koninckii* individuals.

Length of cephalon and transitory pygidium at M0 (ce and p , respectively)

In order to estimate initial size parameters, the length of the cephalon at M0 was set as the intercept of the same regression used to determine the cephalic growth rate (see above and Fig. 1A). Because new tergites were released from the anterior part of the transitory pygidium during the meraspid phase, the average length of the pygidium stayed generally constant (Fig. 1C). Thus the length of the transitory pygidium at M0 was set as the average across all meraspids.

Length of newly released tergite ($t.p$)

This parameter was estimated as the average ratio between the length of the newly released thoracic tergite in each meraspid molt (for all individuals with 17 or fewer tergites) relative to the sum of that length and the length of the pygidium in the same molt (Fig. 1D). It is possible that some of the variation in this ratio across specimens (and that of pygidial length through ontogeny) is due to variation in the number of segments expressed in the transitory pygidium in different individuals with the same number of tergites.

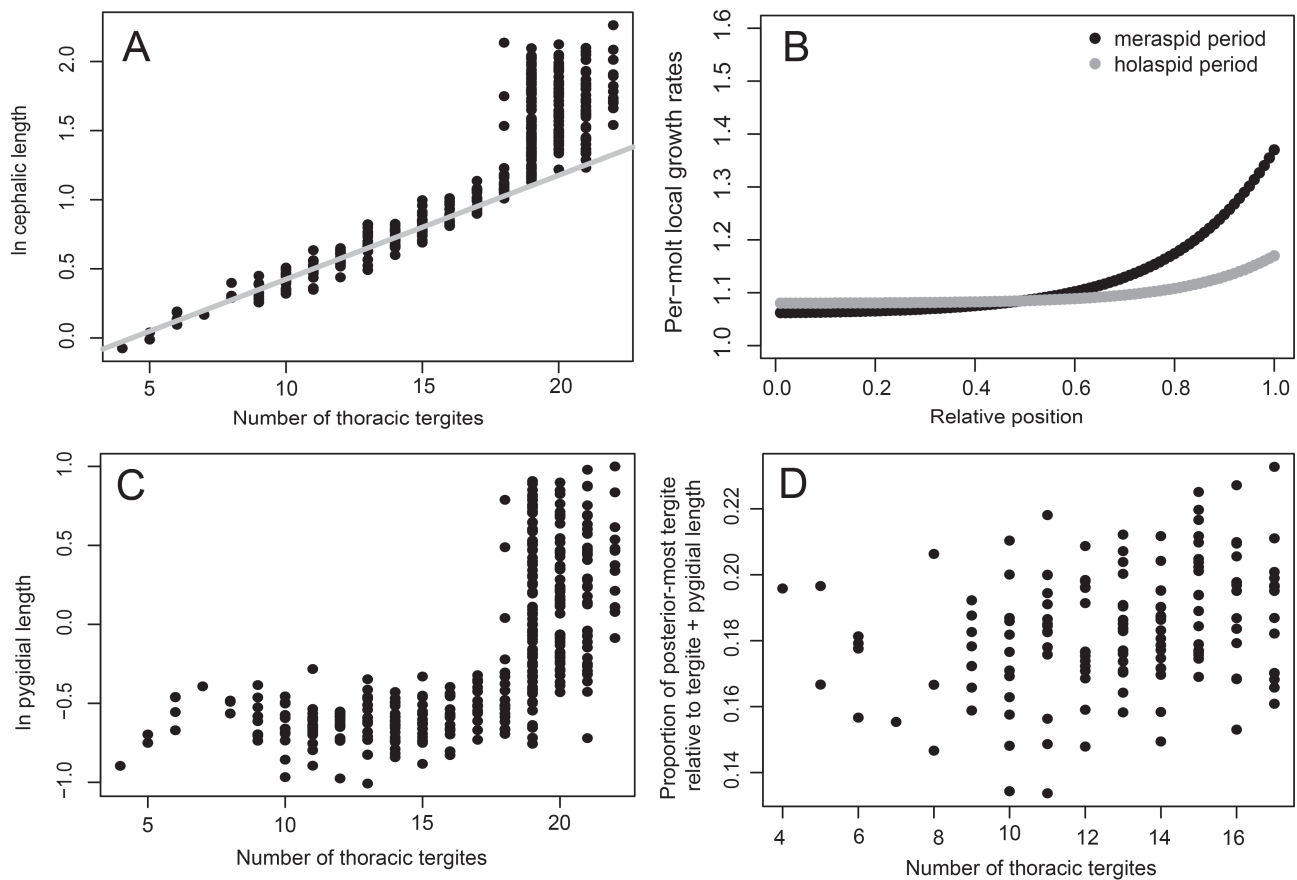


Figure 3. Summary of empirical data used to derive parameter estimates. (A) Lengths of cephalia in *A. koninckii* grouped by number of tergites in the thorax. Because the terminal number of tergites is variable in *A. koninckii*, the regression line was based only on molts which were clearly within the meraspid phase (number of tergites < 18). The rate of cephalic length increase is the exponential of the slope of the regression line. (B) Growth gradients along trunk for *A. koninckii* during the meraspid (black) and holaspid (gray) periods. See [Supplementary Figure S1A](#) for an image of a holaspid *A. koninckii* and Hong et al. (2014) for images of meraspid specimens. (C) Lengths of transitory and adult pygidia in *Aulacopleura koninckii*, grouped by the number of tergites in the exoskeleton. The terminal number of tergites was variable in *A. koninckii* (ranging from 18 to 22), which is why the average length and range of length measurements increases dramatically if there are 18 or more thoracic tergites. Note that the size of the transitory pygidium does not change significantly during the meraspid period although there may have been increases and decreases over ontogeny. (D) Proportion of the length of the “pygidial” part of the trunk that is expressed as the newly-released tergite in *A. koninckii*. Although the number of segments in each transitory pygidium varies in *A. koninckii*, there is no relationship between the length of the pygidium and the number of segments for any meraspid molt ([Fig. S3](#)).

However, there is no consistent relationship between the number of segments in the transitory pygidium and its length ([Fig. S3](#)).

Number of molts during which initial or “meraspid” growth gradient is active (R)

This parameter is set to equal the number of molts during the meraspid period (T_{er}), consistent with a trilobite that is synanthromeric.

Output of the model for *Aulacopleura koninckii*

The output of the model is the estimated lengths of each dorsal sclerite at each molt. The output after applying the parameters calculated from measurements of *Aulacopleura koninckii* is shown in [Figure 4](#).

Modeled body sizes and body proportions are similar to empirical data for *A. koninckii* (Table 2), and if the model is run five times for each terminal number of thoracic tergites (T_{er}) from 18 to 22, the resulting total body sizes are consistent with the variation in body size in the empirical dataset (Fig. 5). However, in the model output, the length of the thoracic tergites decrease posteriorly in the trunk at all molt stages. In the empirical dataset, the length of the first four or five thoracic tergites tends to increase posteriorly before decreasing to the pygidium (there is variation in this, but it is not clear how much might be due to measurement error), a pattern that has been seen in other trilobites as well.

Table 2. Comparison of length estimates from model to length estimates from empirical data (Hughes et al., 2017). Assuming a constant cephalic growth rate, the largest specimen with 20 tergites in the empirical dataset is estimated to have molted 31 times (based on OLS regression of $\log(\text{cephalic size})$ on molt stage in juveniles) and should be comparable to the model output at molt 31.

Length	Model output (mm)	Mean (standard deviation, range) from empirical data (mm)
Cephalon, molt 9	1.40	1.42 (0.10, 1.29–1.57)
Cephalon, molt 14	2.10	2.06 (0.13, 1.82–2.29)
Cephalon, maximum	8.40	8.36
Transitory pygidium, molt 9	0.46	0.56 (0.07, 0.48–0.68)
Transitory pygidium, molt 14	0.52	0.54 (0.06, 0.43–0.65)
Pygidium, maximum	3.02	2.46
Thorax, molt 9	1.49	1.30 (0.08, 1.19–1.47)
Thorax, molt 14	2.92	2.52 (0.16, 2.28–2.99)
Thorax, maximum	16.06	13.90
Total body size, molt 9	3.35	3.28 (0.23, 3.02–3.72)
Total body size, molt 14	5.54	5.11 (0.30, 4.65–5.80)
Total body size, maximum	27.48	24.72

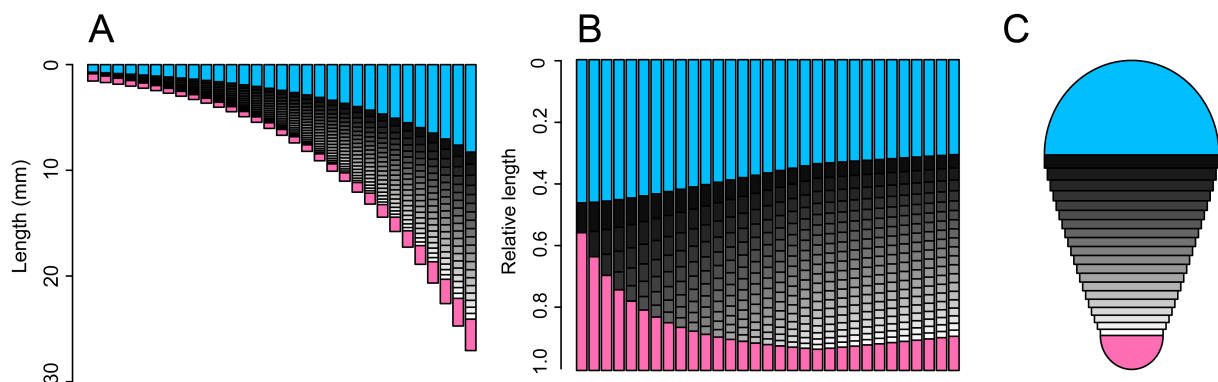


Figure 4. Model results. Estimated (A) and relative lengths (B) of dorsal sclerites for each molt (up to molt 31) when model is run using the parameter values estimated from specimens of *Aulacopleura koninckii* (Table 1). Each column represents a trilobite at a different growth stage. The columns are arranged from earliest stage on the left to latest stage on the right. The blue section of each column represents the length of the cephalon, the gray-colored sections represent the thoracic tergites, and the pink section represents the length of the pygidium. Note that the pygidium is at its smallest size relative to the length of the cephalon at the transition between the meraspid and holaspid stages. (C) Schematic of trilobite body at molt 31; width of cephalon and pygidium set to be twice the length.

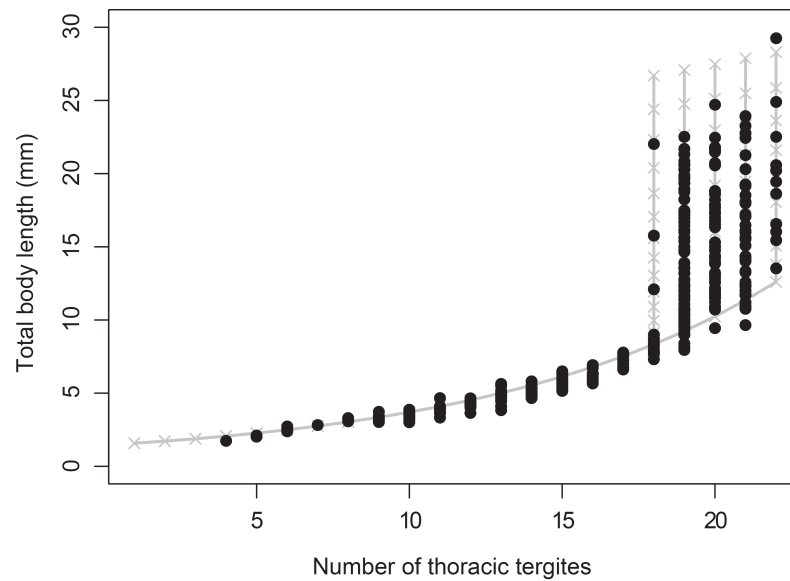


Figure 5. Comparison of total body size for *Aulacopleura koninckii* specimens in the dataset of Hughes et al. (2017) with model output for terminal number of thoracic tergites varying from 18 to 22. Gray crosses = body size at each time step of the model, shown for all five model runs, with gray lines connecting them to aid visualization. Black dots = empirical measurements of body size in *A. koninckii*. The specimen shown in Supplementary Figure S1A is on the small end of the range of body sizes for specimens with 19 thoracic tergites, making it a “young” holaspid.

Parameter variation and resulting relative growth

The relative length of different sclerites, as well as maximum body size, may be explored by varying different parameters.

Influence of varying the initial cephalic and pygidial length

It is likely that there was variation in the size of the cephalon and transitory pygidium at M0. In order to capture the influence of this variation on total body length, the initial cephalic and pygidial lengths were sampled from normal distributions with means of 0.67 and 0.55, respectively, and standard deviations of 0.05. When the lengths of the cephalon and transitory pygidium at M0 are allowed to vary, the variance in body size at any given molt increases throughout growth, unlike the variance in body size in the empirical dataset, most notably at later molt stages (Fig. 6). This puts a fine point on the fact that there is no canalization mechanism built into the current model (see Hughes et al., 2017 for discussion of growth canalization). At the latest molt stages, the median body size in the empirical dataset is consistently lower than the median from the model output. Although within the range possible if initial cephalic and pygidial lengths varied, this suggests that growth rates may have slowed late in life in a way not captured by the current model.

Influence of varying the terminal number of thoracic tergites

If no other parameters are changed, one might expect that reducing the number of tergites will result in smaller trilobites. This is true, but the decrease is small. For example, decreasing the terminal number of thoracic tergites by 50% ($T_{er} = 10$) results in a trilobite that is only 85% smaller (Fig. 7). Because the cephalon is growing at the same rate, it is the relative proportions of the trunk that vary to accommodate this. In particular, the relative length of the pygidium is much greater in a trilobite with fewer thoracic tergites because the pygidium is under positive growth (during which it no longer releases tergites into

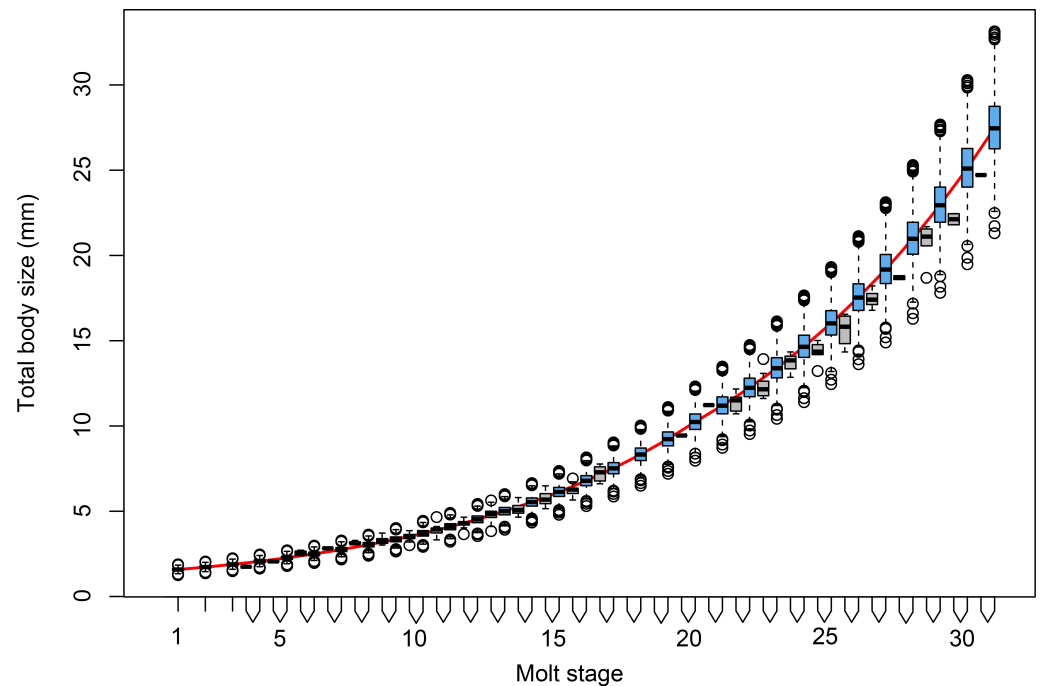


Figure 6. Variation in total body length at different stages when the lengths of the M0 cephalon and transitory pygidium are allowed to vary (blue boxplots). Red line = model output when *ce* and *p* are set to estimated values in Table 1. Shown to the left of the model results are the body size measurements from the *A. koninckii* dataset for all meraspids and holaspids with 20 thoracic tergites.

the thorax) for a greater proportion of the lifespan. In addition, any particular tergite numbered from the front (e.g., the second tergite) will undergo a relatively higher growth rate throughout the lifespan because it shares a larger portion of the growth gradient. However, smaller (and re-proportioned) trilobites would result if there was a limit on the total number of molts the trilobite underwent during holaspis ($Molt < 31$) rather than a constant total number of molts during the entire lifespan.

Influence of increasing rates systematically across body regions

It should be possible to generate a smaller or larger trilobite without altering body proportions if rates are adjusted systematically across all body regions. To determine the sensitivity of body size to changes in rates, the cephalic growth rate (*g.c*) and the minimum and maximum growth rates of the trunk region (*lowM*, *highM*, *lowH*, *highH*) were systematically adjusted and the model re-run. A four-percent increase in the rates across these five parameters resulted in a trilobite that is 3.5 times larger than before but with the same relative body proportions (Table 3).

Influence of varying the growth gradient during meraspis or holaspis

In *A. koninckii*, the growth gradient becomes shallower at the transition from the meraspid period to the holaspid period, due to an increase in the minimum and decrease in the maximum rates (Fig. 3B).

The maximum rates along the growth gradient (*highM*, *highH*) primarily affect growth of the pygidium, and this transition also marks the point in growth where the pygidium actively increases in size because tergites are no longer being released into the thorax. Thus, one way to make an isopygous trilobite (one where the pygidium is of equal length to the cephalon) is to maintain the high growth rate at the posterior part of the trunk into holaspis, for example by retaining the meraspid growth gradient through holaspis (Fig. 8). One interesting result is that the length of the thoracic tergites decreases and

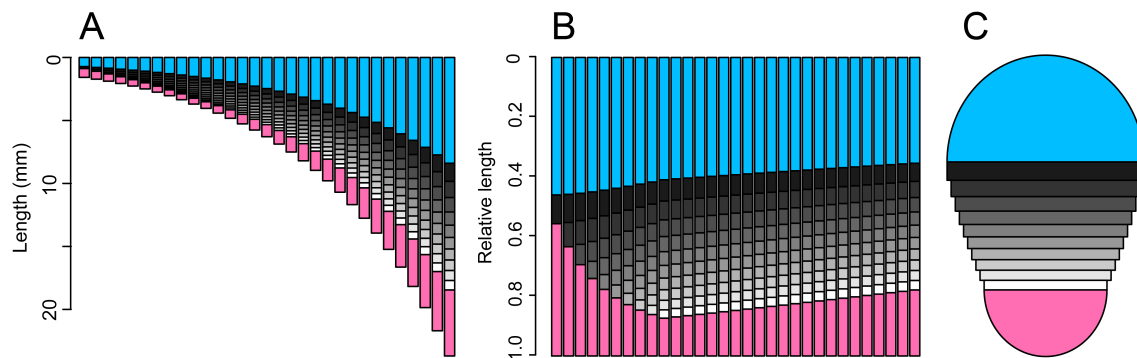


Figure 7. Model results when terminal number of thoracic tergites is varied. Estimated (A) and relative lengths (B) of dorsal sclerites for each molt (up to molt 31) when terminal number of tergites is decreased to 10 (all other parameters as in Table 1). (C) Schematic of trilobite body at molt 31; width of cephalon and pygidium set to be twice the length. Compared to *A. koninckii* with 20 tergites (Fig. 4; Table 2), the maximum body size (23.70 mm) is similar. Specifically, the trunk length is slightly decreased with much of the total length redistribution to the pygidium. The average tergite length is also longer. For color explanation, see Figure 4.

Table 3. Increase in total body size if growth parameters are systematically increased. The cephalic and pygidial lengths are relative to the total body size.

Proportional change in each parameter	<i>g.c</i>	<i>lowM</i>	<i>highM</i>	<i>lowH</i>	<i>highH</i>	Total body size (mm)	Relative cephalic length	Relative pygidial length
1	1.085	1.060	1.370	1.084	1.168	27.48	0.306	0.110
1.01	1.096	1.070	1.383	1.095	1.180	37.41	0.306	0.110
1.04	1.128	1.102	1.425	1.127	1.215	92.69	0.306	0.110
0.99	1.074	1.049	1.356	1.073	1.156	20.12	0.306	0.110
0.96	1.042	1.017	1.315	1.040	1.121	7.75	0.306	0.110

then increases posteriorly in the latest molt stages. The pygidium will eventually outgrow the cephalon if λ is increased during the holaspis period, which would decrease the concavity of the exponential decay curve and result in higher growth rates across a larger area of the posterior part of the trunk.

The holapsis growth curve in *A. koninckii* is shallow enough along most of the trunk that the relative length of the thorax may remain almost constant during holaspis (Figs 4, 7). As the range of the growth gradient is decreased, the exponential curve becomes more and more similar to a horizontal line. This ultimately results in true isomorphic growth along the trunk (i.e., constant rates rather than a growth gradient) (Fig. 9). Because of the shape of the exponential decay curve, a constant rate near the lower end of the growth gradient (1.084 for *A. koninckii*) yields a total body length closest to that of actual specimens, but the relative length of the pygidium to the cephalon is smaller. Further, because the minimum growth rate of the trunk (*lowH*) is almost exactly the same as the cephalic growth rate, the relative proportions of the cephalon, thorax, and pygidium will remain constant during holaspis when the holaspis rates are constant and low (Fig. 9G–I).

Influence of decoupling between timing of shift in growth gradients and termination of tergite release

Because the growth gradient is shallower and has a smaller maximum rate during holaspis than during meraspis (at least in *A. koninckii*), altering the timing of transition between growth gradients has differential effects depending on whether the transition between growth gradients occurs before or after termination of tergite release (Fig. 10; Table 4). If the transition happens earlier in ontogeny relative to the termination

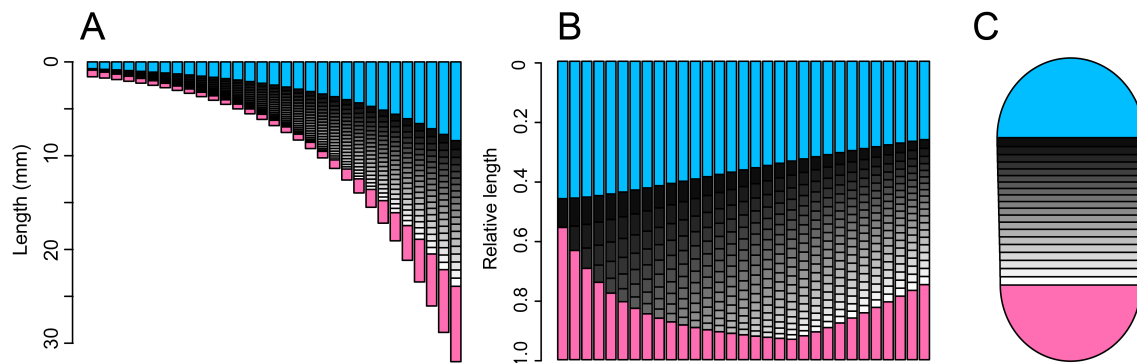


Figure 8. Model results if maximum growth rates near the posterior part of the trunk are maintained at higher values into the holaspid period. Here this is achieved by applying the same growth gradient in meraspid and holaspid periods ($lowM = lowH = 1.060$; $highM = highH = 1.370$; $lambdaM = lambdaH = -5.001$). **(A)** Estimated lengths of sclerites. **(B)** Relative lengths of sclerites. **(C)** Schematic of trilobite body at molt 31; width of cephalon and pygidium set to be twice the length. For color explanation, see Figure 4.

of tergite release, the total exoskeletal length is slightly smaller because rates decrease sooner but the pygidium is much smaller because tergite release continues even though the pygidium grows at a slower rate. In contrast, if the transition happens later in ontogeny relative to the termination of tergite release, the total exoskeletal length is slightly larger but the pygidium is much larger because high growth rates continue even after tergites are no longer being released. The change in relative proportions would not be as great if new segment generation occurred in the thorax as opposed to the pygidium.

Table 4. Comparison of exoskeletal proportions when growth gradient shift occurs before, coincident with, or after termination of tergite release into the thorax. In this example, termination of tergite release occurs at molt 20 ($Ter = 20$). All length measurements are standardized to $R = 20$ ($R = Ter$).

R	Relative total length	Relative length of thorax	Relative length of pygidium
15 ($R << Ter$)	0.928	0.960	0.559
18 ($R < Ter$)	0.963	0.986	0.740
20 ($R = Ter$)	1	1	1
22 ($R > Ter$)	1.017	0.990	1.214
24 ($R >> Ter$)	1.044	0.967	1.574

How many specimens are needed to estimate growth parameter?

The *Aulacopleura koninckii* of dataset of Hughes et al. (2017) comprises 351 well-preserved articulated specimens, 40% of which span the ontogeny of the species from meraspid stage 4 to 17 (sample sizes for each stage shown in Supplementary Figure S3). Such a collection of specimens is exceedingly rare, for both taphonomic and practical reasons. Thus, it may be useful to know how many specimens are needed to accurately estimate growth parameters for this and other species, and what level of precision might be expected under different sampling scenarios. Subsampling routines of the *A. koninckii* dataset produced the following results.

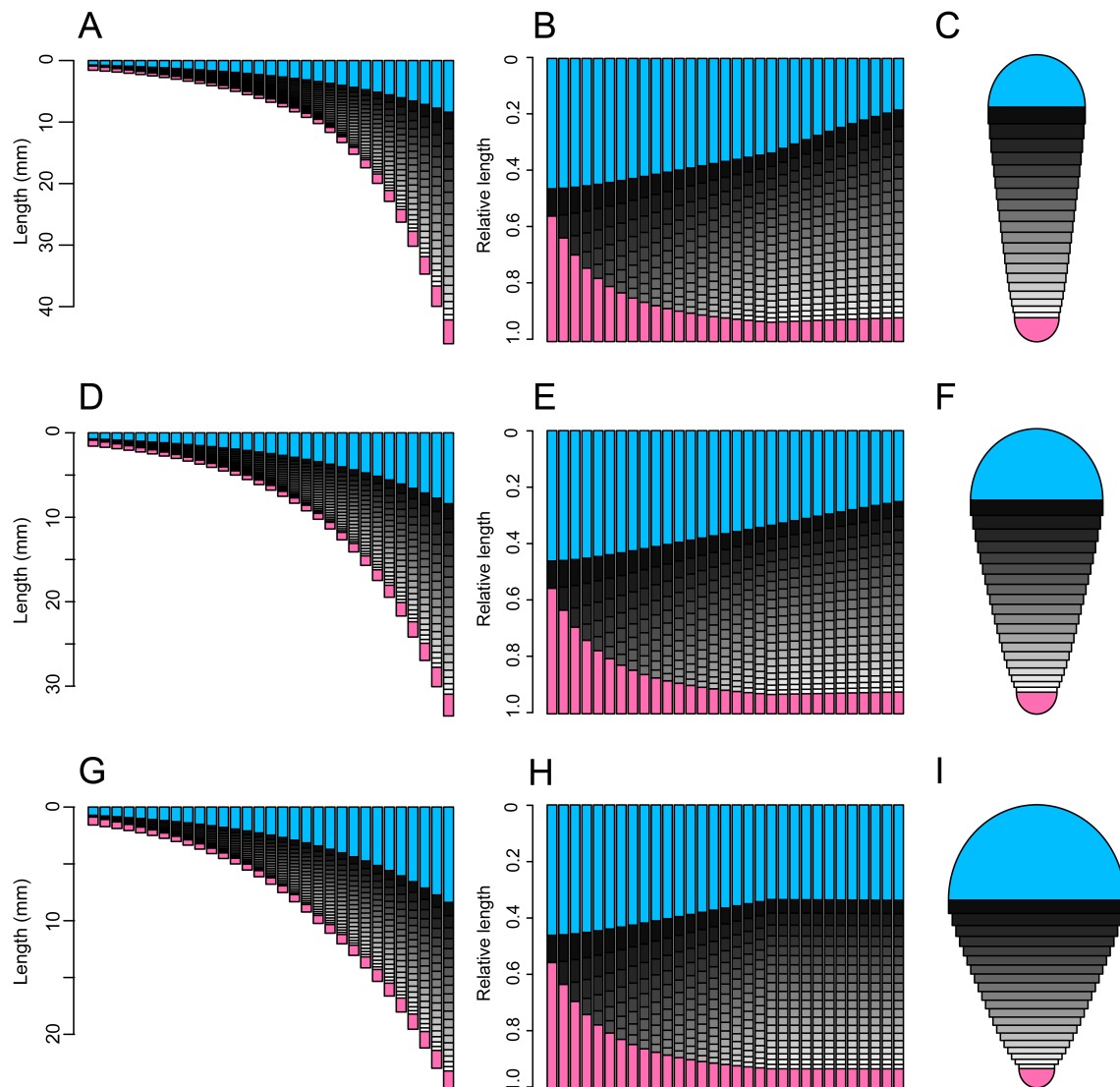


Figure 9. Growth patterns when constant rates are applied across the trunk region during the holaspis period. (A–C) Rates are close to the maximum expressed by *A. koninckii* during the holaspis period ($highH = lowH = 1.168$). (D–F) Rates are the average expressed by *A. koninckii* during the holaspis period ($highH = lowH = 1.125$). (G–I) Rates are the minimum expressed by *A. koninckii* during the holaspis period ($highH = lowH = 1.084$). For color explanation and further information about different columns, see Figure 4.

One specimen per stage

One specimen per stage (M9–M17) was randomly selected from the dataset and the following parameters were estimated: 1) the cephalic length at M0 (ce); 2) the transitory pygidium length at M0 (p); 3) the rate of growth of the cephalon ($g.c$); 4) the proportional size of the newly released tergite at each stage ($t.p$); and 5) the minimum ($lowM$), maximum ($highM$), and exponential decay constant ($lambdaM$) describing the growth gradient. This was repeated 1000 times. In each iteration, each stage was represented by one specimen.

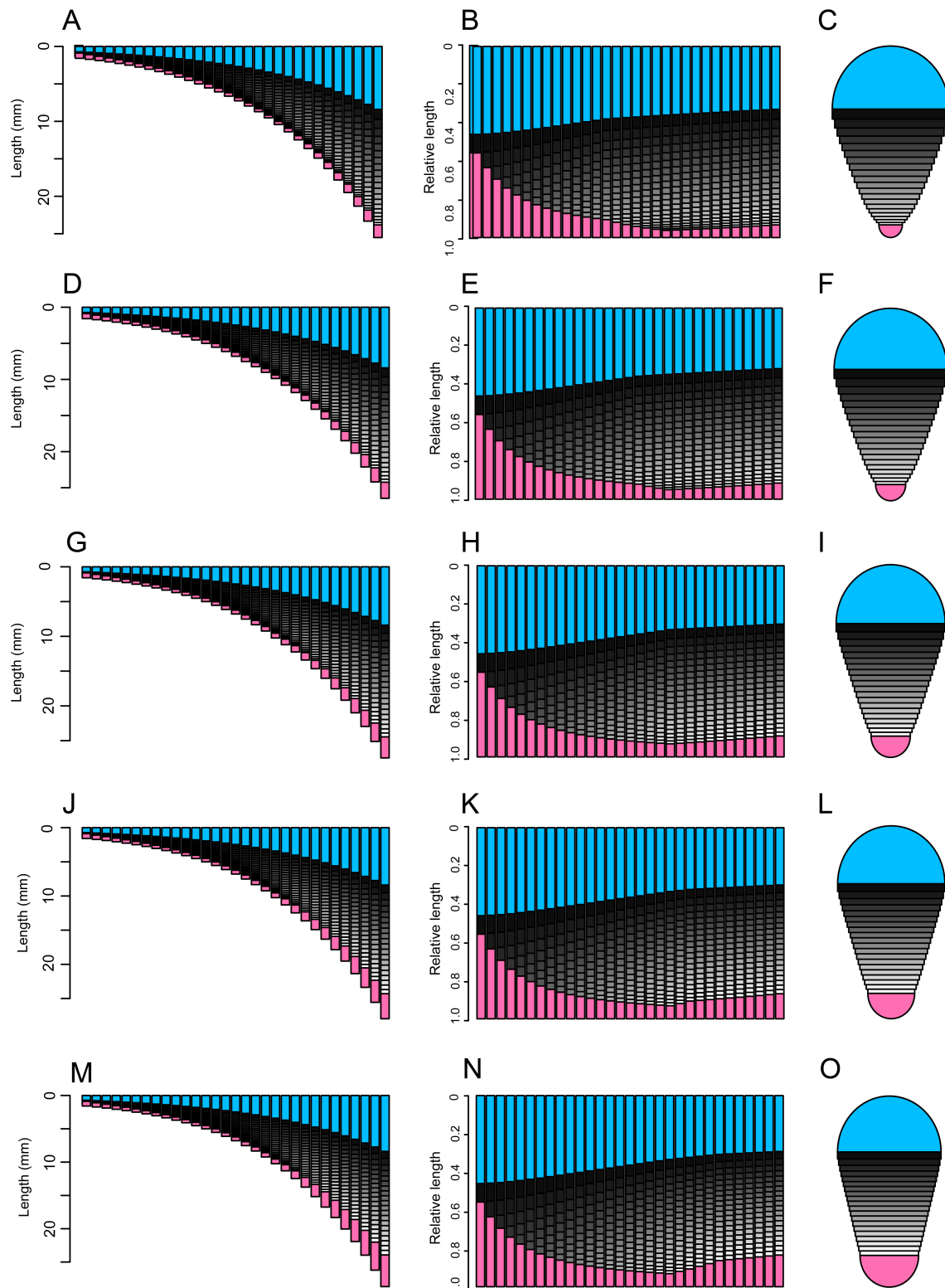


Figure 10. Impact of altering the relative timing of growth gradient transition and termination of tergite release into the thorax on body size and relative proportions. In all panels, termination of tergite release occurs at molt 20, but the transition from the initial growth gradient to the mature growth gradient R occurs in molt 15 (A–C), molt 18 (D–F), molt 20 (G–I), molt 22 (J–L), and molt 25 (M–O). The total exoskeletal length gets slightly longer going from the top to bottom panels but the relative proportion of the pygidium gets much longer at the expense of the total length of the thorax (the rate of cephalic growth is constant in all iterations). See also Table 3. For color explanation, see Figure 4.

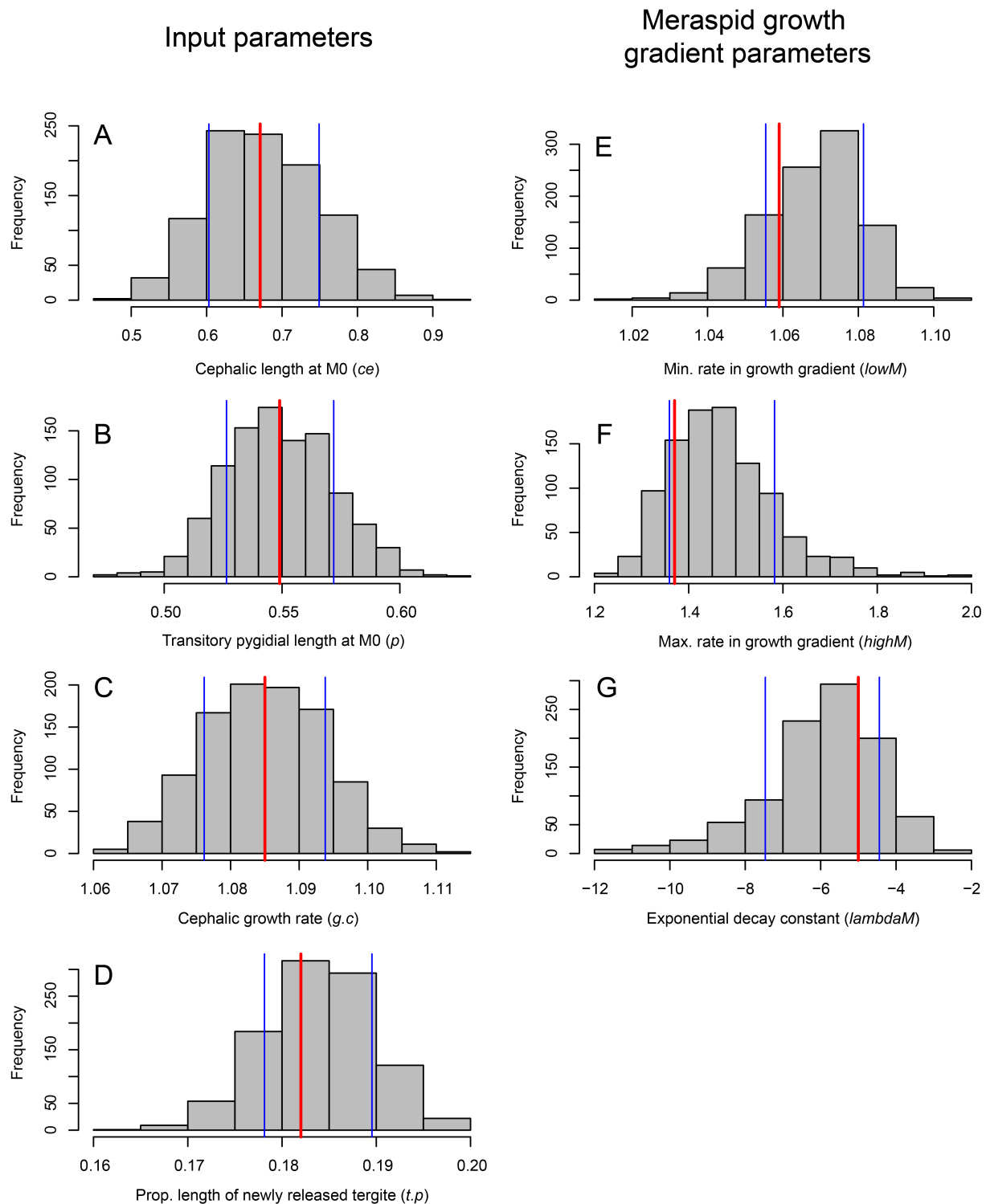


Figure 11. Parameters estimates using one specimen per stage. Parameters estimates for cephalic length at M0 (**A**), transitory pygidial length at M0 (**B**), cephalic growth rate (**C**), proportional length of newly released tergite (**D**), minimum rate in growth gradient (**E**), maximum rate in growth gradient (**F**), and exponential decay constant (**G**), calculated from subsets of *A. koninckii* specimens (one from each stage from M9 to M17). Blue lines show one standard deviation around the mean across all subsampled datasets. Red line shows the parameter estimated from the entire dataset (Table 1). For the growth gradient parameters, extreme outliers have been excluded: only maximum rates less than 2.0 (comprising 98.9% of the subsampling results) are shown; only exponential decay constants greater than -12 (comprising 98.5% of the subsampling results) are shown. See Figure 12 for complete ranges in estimates at low sample sizes.

All of the input parameters (ce , Fig. 11A; p , Fig. 11B; $g.c$, Fig. 11C; $t.p$, Fig. 11D) are well estimated, while the minimum and maximum growth rates in the trunk ($lowM$, Fig. 11E; $highM$, Fig. 11F) tend to be overestimated, and the exponential decay constant tends to be underestimated ($lambdaM$, Fig. 11G). The result of this imprecision on input parameters is expected to be small, given that impact on total body size of varying the initial cephalic and pygidial length (ce and p) using a higher standard deviation (Fig. 6). However, the ranges of values for the growth gradient parameters is high: even excluding the extreme outliers, the range of values is greater than the difference between the meraspid and holaspid growth gradients estimated for *A. koninckii* (Table 1). Given the results of varying these parameters above (Figs 6–10), poor estimates for growth gradient parameters are expected to have a greater impact on model output than poor estimates for input parameters.

More than one specimen per stage

n specimens were randomly selected from each of stages M9–M17, where n ranged from 2 to 8 (8 is the minimum number of specimens representing these stages, see Supplementary Figure S3), and the four input and three meraspid growth parameters were estimated. This was repeated 1000 times. In each iteration, each stage was represented by the same number of specimens. For graphical comparison, univariate density estimates were constructed from the frequency distributions using the `sm.density` function in the R package *sm* ver. 2.2-5.6 (Bowman and Azzalini, 2018).

As expected, with an increase in the number of specimens per stage, the range in parameter estimates decreased (Fig. 12). The mean estimates shifted towards values estimated from the entire empirical dataset, most notably for growth gradient parameters which were more severely over- or underestimated at low sample sizes (Fig. 12E–G). Here, where specimens were being drawn from the latter half of the meraspid period (M9–M17), at least six specimens per meraspid molt stage were needed to accurately estimate parameters describing the growth gradient. For both input and growth gradient parameters, sampling more than six specimens per meraspid growth stage yielded increasingly precise estimates, but with diminishing returns.

A few specimens from few to many stages

n specimens from k stages were randomly selected from the dataset and the four input and three meraspid growth parameters were estimated. For the input parameters, this was repeated 1000 times for each of k ranging from 3 to 14 (representing just three to all stages M4–M17) and for n number of specimens ranging from 3 to 5. Because determining the growth gradient requires a larger sample size (= larger number of molt stages represented), growth parameters were estimated for each of k ranging from 10 to 14 (representing ten to all stages M4–M17). In each iteration, each selected stage was represented by the same number of specimens.

As expected, with an increase in the number of stages represented, the range in parameter estimates decreased (Figs 13, 14). However, there was no shift in the mean estimate of growth gradient parameters as the number of stages represented was increased (Fig. 14). This implies that once many meraspid stages are represented in a sample (> 10), fewer specimens per stage are required to get accurate estimates. The precision was more quickly improved by increasing the number of stages represented than by increasing the number of specimens (within a small range) in each stage (Fig. 14).

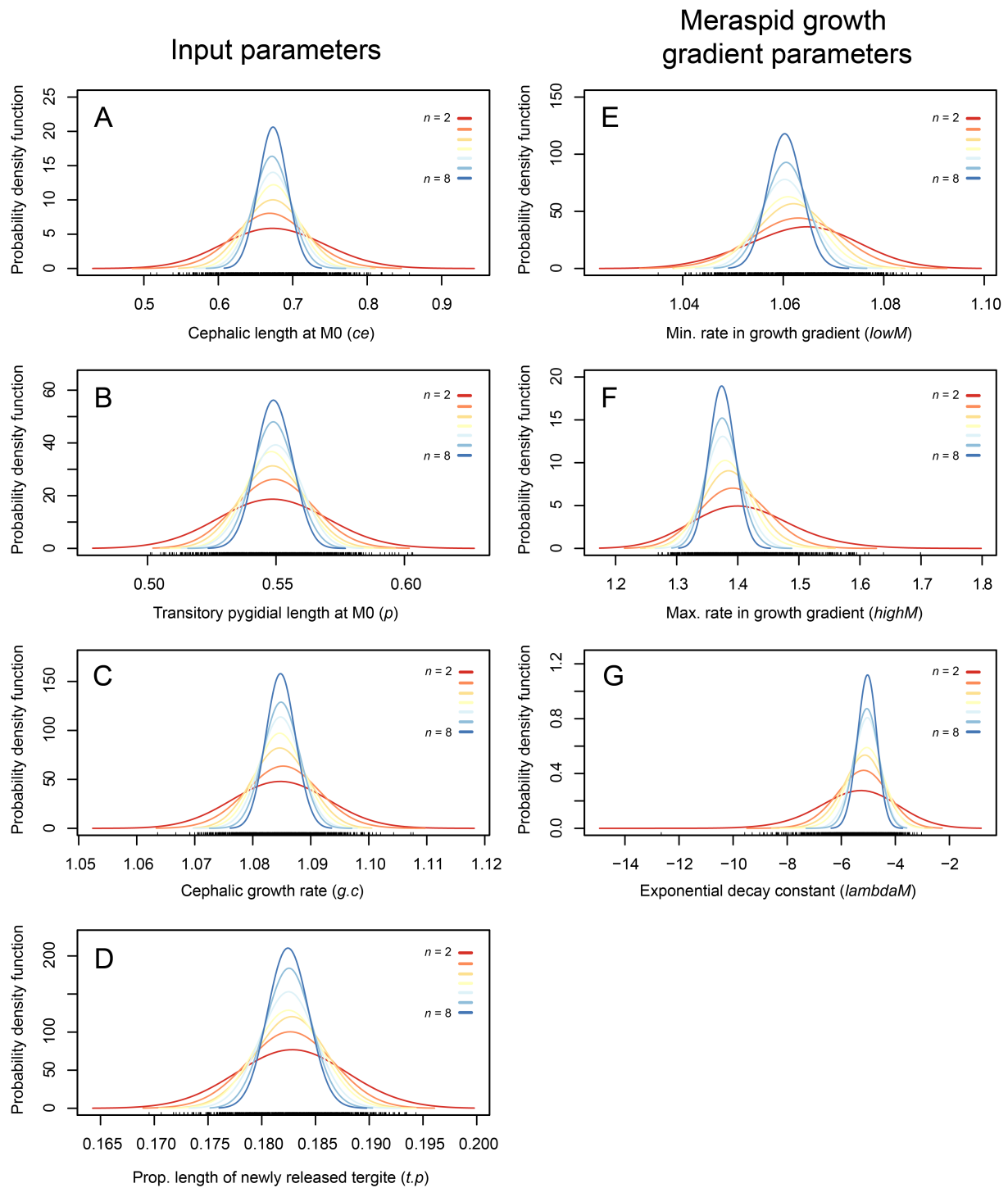


Figure 12. Parameters estimates using more than one specimen per stage. Parameters estimates for cephalic length at M0 (**A**), transitory pygidial length at M0 (**B**), cephalic growth rate (**C**), proportional length of newly released tergite (**D**), minimum rate in growth gradient (**E**), maximum rate in growth gradient (**F**), and exponential decay constant (**G**), calculated from subsets of *A. koninckii* specimens (two to eight specimens from each stage M9 to M17).

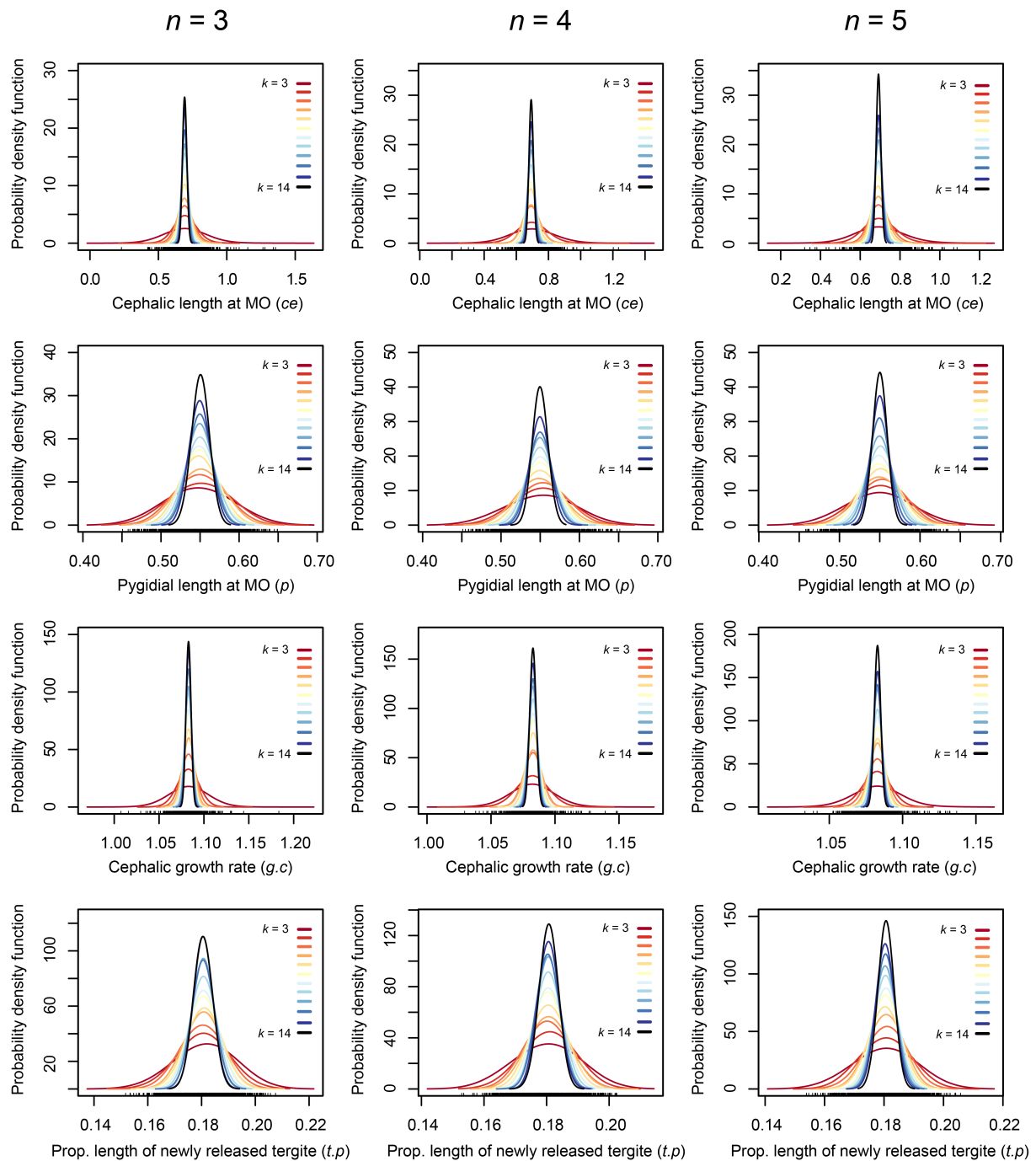


Figure 13. Subsampling results for input parameter estimates when a few specimens (n ranges from 3 to 5) are randomly selected from a few to many (k ranges from 3 to 14) meraspid molt stages.

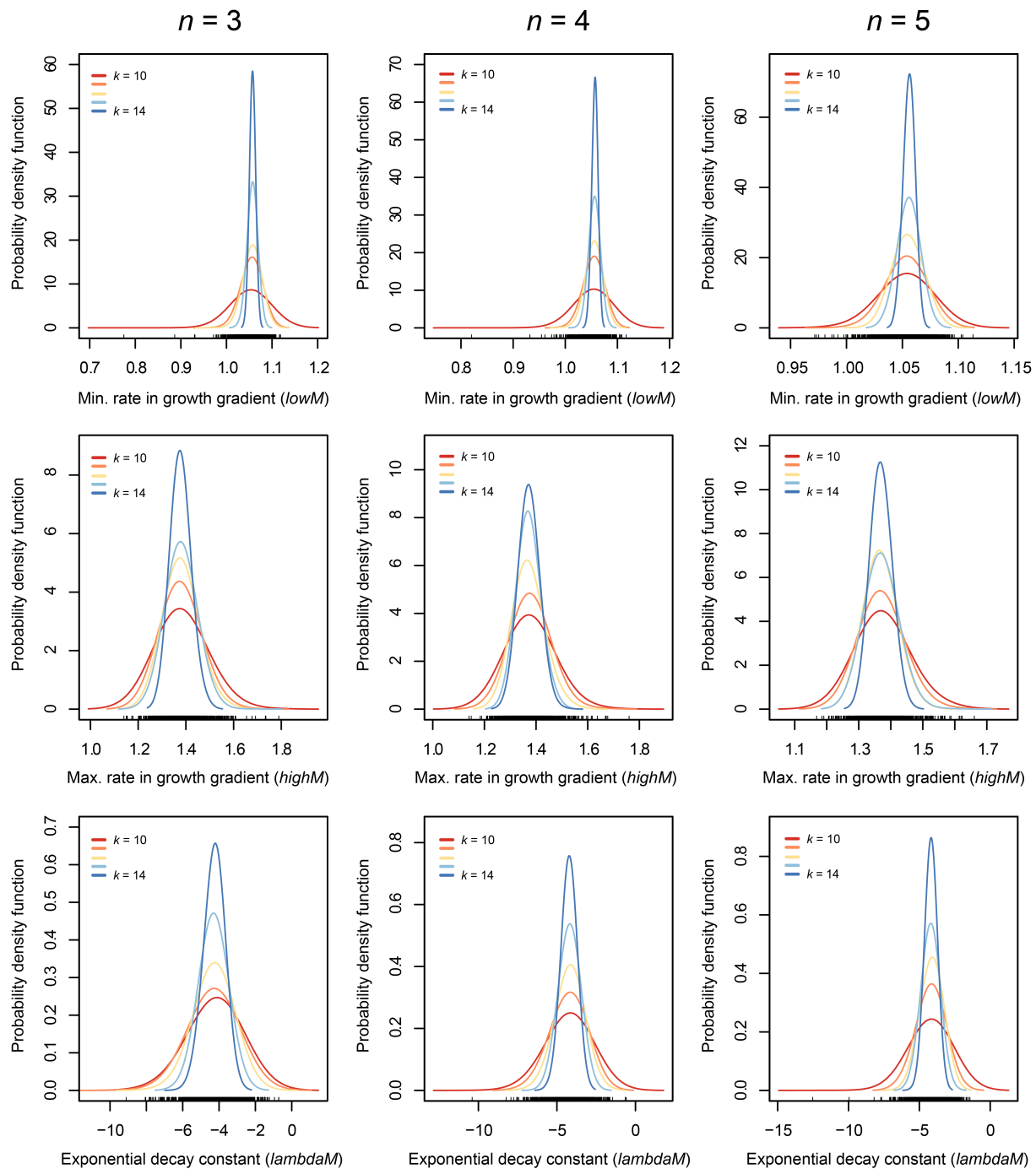


Figure 14. Subsampling results for growth gradient parameters when a few specimens (n ranges from 3 to 5) are selected from several to many (k ranges from 10 to 14) meraspid molt stages.

Implications and applications of the model

With the approach proposed in this paper, a minimum of nine parameters are required to model basic trilobite growth and segmentation, and three additional parameters are required to allow a transition to a new growth gradient for the trunk region during ontogeny. It is possible to add additional parameters to describe additional variation in the segmentation schedule or variation in growth rates throughout ontogeny. As an example herein, the parameter R allows for variation in the timing of the transition to a new growth gradient. Other modifications could include varying the timing of tergite release in the thorax. For example, some trilobites alternated segment generation in the pygidium and segment release into the trunk (Hughes et al., 2006; Hopkins, 2017). Finally, many species may have undergone multiple molt cycles while still in the protaspid period and this could lead to variation in body sizes and the proportion of cephalic to transitory pygidial lengths at the start of the meraspid period. Although this model does not explicitly include the earliest sclerotized developmental stages, the impact of differential growth or growth variation in the protaspid period was approximated by varying the ce and p input parameters, as described above (Fig. 6).

In addition to increasing the complexity of the model to better represent specific or unusual developmental patterns in trilobites, it should also be possible to apply this approach to modeling growth in other arthropods, particularly other hemianamorphic arthropods for which segmentation patterns are known (e.g., conchostracans, Olesen, 1999; copepods, Ferrari and Dahms, 2007). One of the major obstacles in applying this to other arthropods may be the initial estimation of parameters from empirical data, which requires samples comprising multiple specimens from multiple molt stages (although good representation of molt stages will likely be more important than large numbers of specimens within molt stages).

Although this model describes basic growth and segmentation, a diverse array of observed body sizes and relative proportions of body regions can be attained by altering only a few parameters at a time. Many of the examples shown here resemble existing species or groups of species. For example, if maximum growth rates of the trunk are maintained at higher values into the holaspid period, the output shows body proportions consistent with isopygous trilobites, where the cephalon and pygidium are near equal in size (Fig. 8). Many asaphid trilobites show this condition (Fig. S1B). Because most pygidial growth occurs during holaspis, depressing the growth gradient during this period yields body proportions consistent with micropygous trilobites, where the pygidium is much smaller in length and width than the cephalon (Fig. 9G–I), as seen in many olenellid trilobites (Fig. S1C). However, similar body proportions may be produced when the transition to the holaspid growth gradient is initiated before termination of thoracic tergite release (Fig. 10A–C) or when cephalic growth rates are increased relative to the growth gradient across the trunk (not shown). Thus it is possible that specific combinations of body size and proportions may be attainable by more than one combination of model parameters. Most trilobites have body proportions that vary between the micropygous and isopygous conditions (Fig. S1D–F).

Given a set number of molts, small changes in growth rates can have large effects on total body size or relative body proportions. The extent to which such changes (and of this magnitude) are ecologically or evolutionarily possible is an open question. A 50% increase in body size is seen in *Poseidonmimus* ostracods over the last 40 million years in association with a decrease in ocean bottom-water temperatures, and some species exhibit almost this entire range of body size across historic populations (Hunt and Roy, 2006). Because ostracods have determinant growth and a fixed number of molt stages, it seems likely that this body size variation was achieved by changes to per-molt growth rates. However, in arthropods with

indeterminate growth (like trilobites), variation in adult body sizes in response to environmental variation (e.g., temperature, food availability, presence of predators) is often achieved by some combination of changes in magnitude of per-molt increase in body size and changes in molt frequency and/or number of molts per life history phase (Maszczyk and Brzezinski, 2018). Better understanding of growth response to environmental variation in trilobites requires further empirical studies (e.g., comparisons of growth rates in environmentally-separated populations of the same species). In the meantime, the model proposed herein may provide a framework for assessing the range of realized body sizes and body proportions in trilobites, and for revealing possible ways in which body size and body proportions may have evolved.

Acknowledgements

The author would like to thank Giuseppe Fusco, Nigel Hughes, and James Hagadorn for discussion and feedback, Kenneth De Baets and Lukáš Laibl for helpful reviews, and Christian Klug for handling the peer review process.

Additional information

Funding

No external funding sources were required for this work.

Competing interests

The authors declares she has no personal or financial conflict of interest relating to the content of this study. MJH is part of the Managing Board of PCI Paleo, but was not involved in the evaluation of this study.

Data availability

R functions for the growth model and parameter estimation, as well as a modified data file, are available at www.github.com/meljh/trilo-growth.

Complete empirical data set is available from: Hughes NC, Hong PS, Hou J, and Fusco G (2017). The development of the Silurian trilobite *Aulacopleura koninckii* reconstructed by applying inferred growth and segmentation dynamics: A case study in paleo-evo-devo. *Frontiers in Ecology and Evolution* 5, 00037. DOI: 10.3389/fevo.2017.00037 (Open Access).

Supplementary information

- R functions for the growth model and parameter estimation, as well as a modified data file, are available at www.github.com/meljh/trilo-growth
- [Supplementary Figures S1–S3](#) appear at the end of this PDF

References

- Barrande J (1846). *Notice préliminaire sur le système Silurien et les trilobites de Bohême*. Leipzig: Hirschfeld. 96 pp.
- Bowman AW and Azzalini A (2018). *R package 'sm': nonparametric smoothing methods*. Version 2.2–5.6. URL: <http://www.stats.gla.ac.uk/~adrian/sm>.
- Chatterton BDE, Siveter DJ, Edgecombe GD, and Hunt AS (1990). Larvae and relationships of the Calymenina (Trilobita). *Journal of Paleontology* 64, 255–277. DOI: 10.1017/S0022336000018424.
- Ferrari FD and Dahms HU (2007). *Post-embryonic development of the Copepoda*. Crustaceana Monographs 8. Leiden: Brill. 229 pp.
- Fusco G, Garland TJ, Hunt G, and Hughes NC (2012). Developmental trait evolution in trilobites. *Evolution* 66, 314–329. DOI: 10.1111/j.1558-5646.2011.01447.x.
- Fusco G, Hong PS, and Hughes NC (2014). Positional specification in the segmental growth pattern of an early arthropod. *Proceedings of the Royal Society B: Biological Sciences* 281, 20133037. DOI: 10.1098/rspb.2013.3037.
- Fusco G, Hong PS, and Hughes NC (2016). Axial growth gradients across the postprotaspid ontogeny of the Silurian trilobite *Aulacopleura koninckii*. *Paleobiology* 42, 426–438. DOI: 10.1017/pab.2016.5.
- Fusco G and Minelli A (2013). Arthropod segmentation and tagmosis. In: *Arthropod Biology and Evolution: molecules, development, morphology*. Ed. by Minelli A, Boxshall G, and Fusco G. Berlin, Heidelberg: Springer-Verlag, pp. 197–221.
- Hong PS, Hughes NC, and Sheets HD (2014). Size, shape, and systematics of the Silurian trilobite *Aulacopleura koninckii*. *Journal of Paleontology* 88, 1120–1138. DOI: 10.1666/13-142.
- Hopkins MJ (2017). Development, trait evolution, and the evolution of development in trilobites. *Integrative and Comparative Biology* 57, 488–498. DOI: 10.1093/icb/icx033.
- Hopkins MJ and Pearson JK (2016). Non-linear ontogenetic shape change in *Cryptolithus tessellatus* (Trilobita) using three-dimensional geometric morphometrics. *Palaeontologia Electronica* 19.3.42A, 1–54. DOI: 10.26879/665.
- Hughes NC (2005). Trilobite construction: building a bridge across the micro- and macroevolutionary divide. In: *Evolving Form and Function: Fossils and Development: Proceedings of a symposium honoring Adolf Seilacher for his contributions to paleontology, in celebration of his 80th birthday*. Ed. by Briggs DEG. New Haven: Peabody Museum of Natural History, Yale University, pp. 139–158.
- Hughes NC (2003a). Trilobite body patterning and the evolution of arthropod tagmosis. *BioEssays* 25, 386–395. DOI: 10.1002/bies.10270.
- Hughes NC (2003b). Trilobite tagmosis and body patterning from morphological and developmental perspectives. *Integrative and Comparative Biology* 43, 185–206. DOI: 10.1093/icb/43.1.185.
- Hughes NC (2007). The evolution of trilobite body patterning. *Annual Review of Earth and Planetary Sciences* 35, 401–434. DOI: 10.1146/annurev.earth.35.031306.140258.
- Hughes NC, Hong PS, Hou J, and Fusco G (2017). The development of the Silurian trilobite *Aulacopleura koninckii* reconstructed by applying inferred growth and segmentation dynamics: A case study in paleo-evo-devo. *Frontiers in Ecology and Evolution* 5, 00037. DOI: 10.3389/fevo.2017.00037.
- Hughes NC, Minelli A, and Fusco G (2006). The ontogeny of trilobite segmentation: a comparative approach. *Paleobiology* 32, 602–627. DOI: 10.1666/06017.1.
- Hunt G and Roy K (2006). Climate change, body size evolution, and Cope's Rule in deep-sea ostracodes. *Proceedings of the National Academy of Sciences* 103, 1347–1352. DOI: 10.1073/pnas.0510550103.
- Maszczyk P and Brzezinski T (2018). Body size, maturation size, and growth rate of crustacean. In: *The Natural History of the Crustacea*. Ed. by Wellborn GA and Thiel M. Vol. 5, Life Histories. Oxford: Oxford University Press, pp. 35–65.

- McGhee GR (1999). *Theoretical morphology: the concept and its applications*. New York: Columbia University Press. 316 pp.
- McGhee GR (2015). Limits in the evolution of biological form: a theoretical morphologic perspective. *Interface Focus* 5, 20150034. DOI: 10.1098/rsfs.2015.0034.
- Minelli A and Fusco G (2013). Arthropod post-embryonic development. In: *Arthropod Biology and Evolution: molecules, development, morphology*. Ed. by Minelli A, Boxshall G, and Fusco G. Berlin, Heidelberg: Springer-Verlag, pp. 91–122. DOI: 10.1007/978-3-662-45798-6_5.
- Minelli A, Fusco G, and Hughes NC (2003). Tagmata and segment specification in trilobites. *Special Papers in Palaeontology* 70, 31–43.
- Olesen J (1999). Larval and post-larval development of the branchiopod clam shrimp *Cyclestheria hislopi* (Baird, 1859) (Crustacea, Branchiopoda, Conchostraca, Spinicaudata). *Acta Zoologica* 80, 163–184. DOI: 10.1046/j.1463-6395.1999.80220015.x.
- Ortega-Hernández J and Brena C (2012). Ancestral patterning of tergite formation in a centipede suggests derived mode of trunk segmentation in trilobites. *PLoS ONE* 7, e52623. DOI: 10.1371/journal.pone.0052623.
- Raup DM (1961). The geometry of coiling in gastropods. *Proceedings of the National Academy of Sciences* 47, 602–609. DOI: 10.1073/pnas.47.4.602.
- Raup DM (1966). Geometric analysis of shell coiling: general problems. *Journal of Paleontology* 40, 1178–1190.
- Thomas AT and Holloway DJ (1988). Classification and phylogeny of the trilobite order Lichida. *Philosophical Transactions of the Royal Society B: Biological Sciences* 321, 179–262. DOI: 10.1098/rstb.1988.0093.
- Thompson DAW (1942). *On Growth and Form: The Complete Revised Edition*. Cambridge: Cambridge University. 1116 pp.
- Urdu S (2015). Theoretical modelling of the molluscan shell: What has been learned from the comparison among molluscan taxa? In: *Ammonoid Paleobiology: From anatomy to ecology*. Ed. by Klug C, Korn D, De Baets K, Kruta I, and Mapes RH. Vol. 43. Dordrecht: Springer Netherlands, pp. 207–251. DOI: 10.1007/978-94-017-9630-9_6.
- Urdu S, Goudemand N, Bucher H, and Chirat R (2010). Allometries and the morphogenesis of the molluscan shell: a quantitative and theoretical model. *Journal of Experimental Zoology Part B: Molecular and Developmental Evolution* 314B, 280–302. DOI: 10.1002/jez.b.21337.
- Whittington HB (2002). Lichidae (Trilobita): morphology and classification. *Journal of Paleontology* 76, 306–320. DOI: 10.1017/S002233600004172X.
- Wilmot NV and Fallick AE (1989). Original mineralogy of trilobite exoskeletons. *Palaeontology* 32, 297–304.

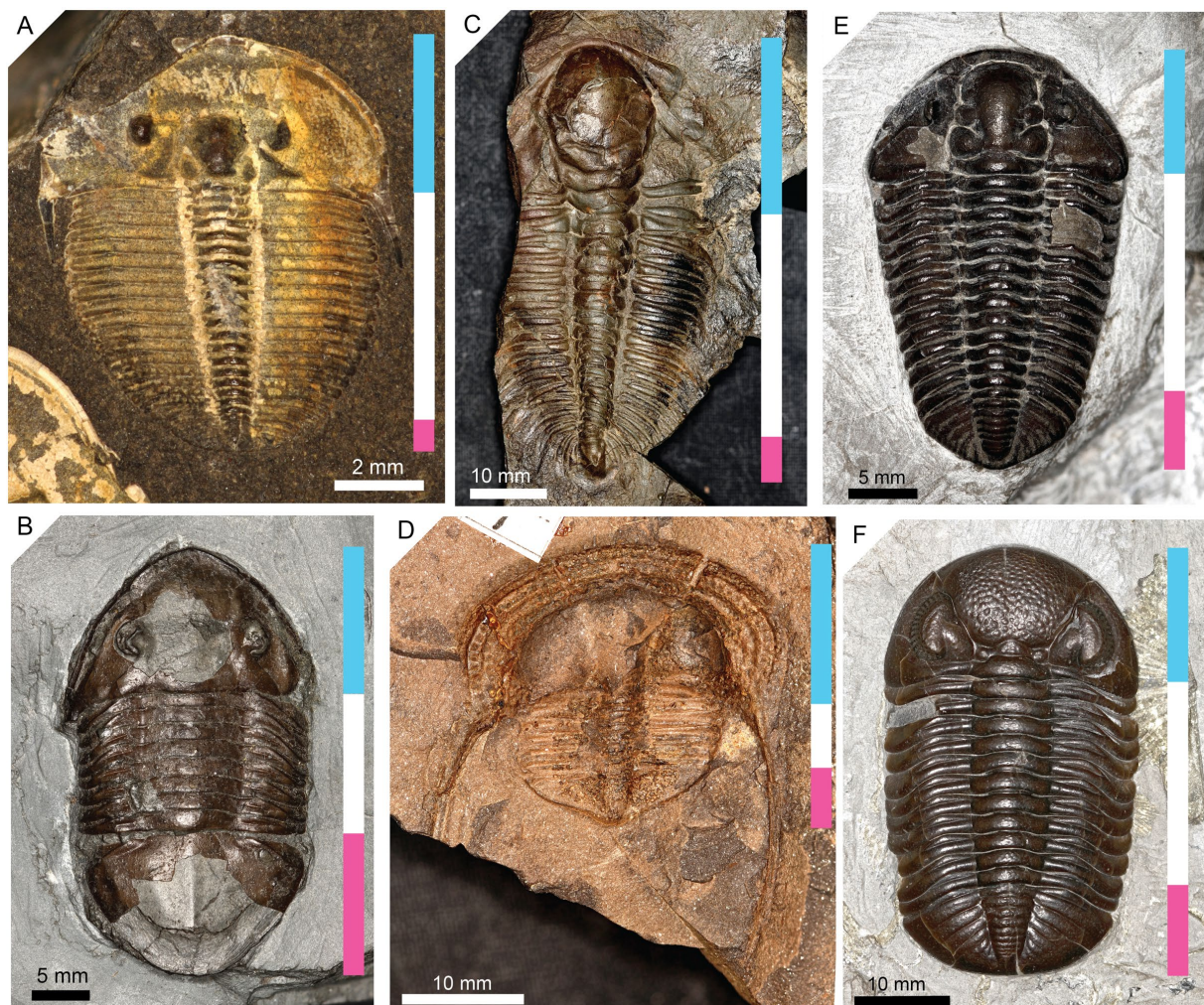


Figure S1. Examples of trilobite species representing some of the diversity in body proportions. (A) *Aulacopleura koninckii* (AMNH-FI-44122) with 19 thoracic tergites. This specimen is only 9.3 mm long, which is amongst the smallest specimens for this number of tergites (Fig. 5), and compared to other specimens on the species, this represents a young holaspid. At this point in the ontogeny, the length of the pygidium relative to the cephalon is the smallest it would be, and it would start to increase as the individual continued to molt (Fig. 4). (B) *Isotelus maximus* (AMNH-FI-68725) with eight thoracic tergites. The specimen is 36.2 mm long, with each body section (cephalon, thorax, and pygidium) representing a third of the total length. (C) *Hydrocephalus minor* (AMNH-FI-135959) with fifteen thoracic tergites. Note the exceptionally small pygidium (both in width and length); this is the classic “micropygous” condition. (D) *Deanaspis seftenbergi*? (AMNH-FI-13232/1) with six thoracic tergites. The pygidium is small relative the cephalon but wide enough that the exoskeleton would not be considered “micropygous” in the strict sense. Note that the cephalon is so large that it comprises half the total body size. (E) *Calymene niagarensis* (AMNH-FI-68743) with thirteen thoracic tergites. (F) *Eldredgeops rana* (AMNH-FI-74982) with eleven thoracic tergites. Blue = length of the cephalon; white = length of the thorax; pink = length of the pygidium.

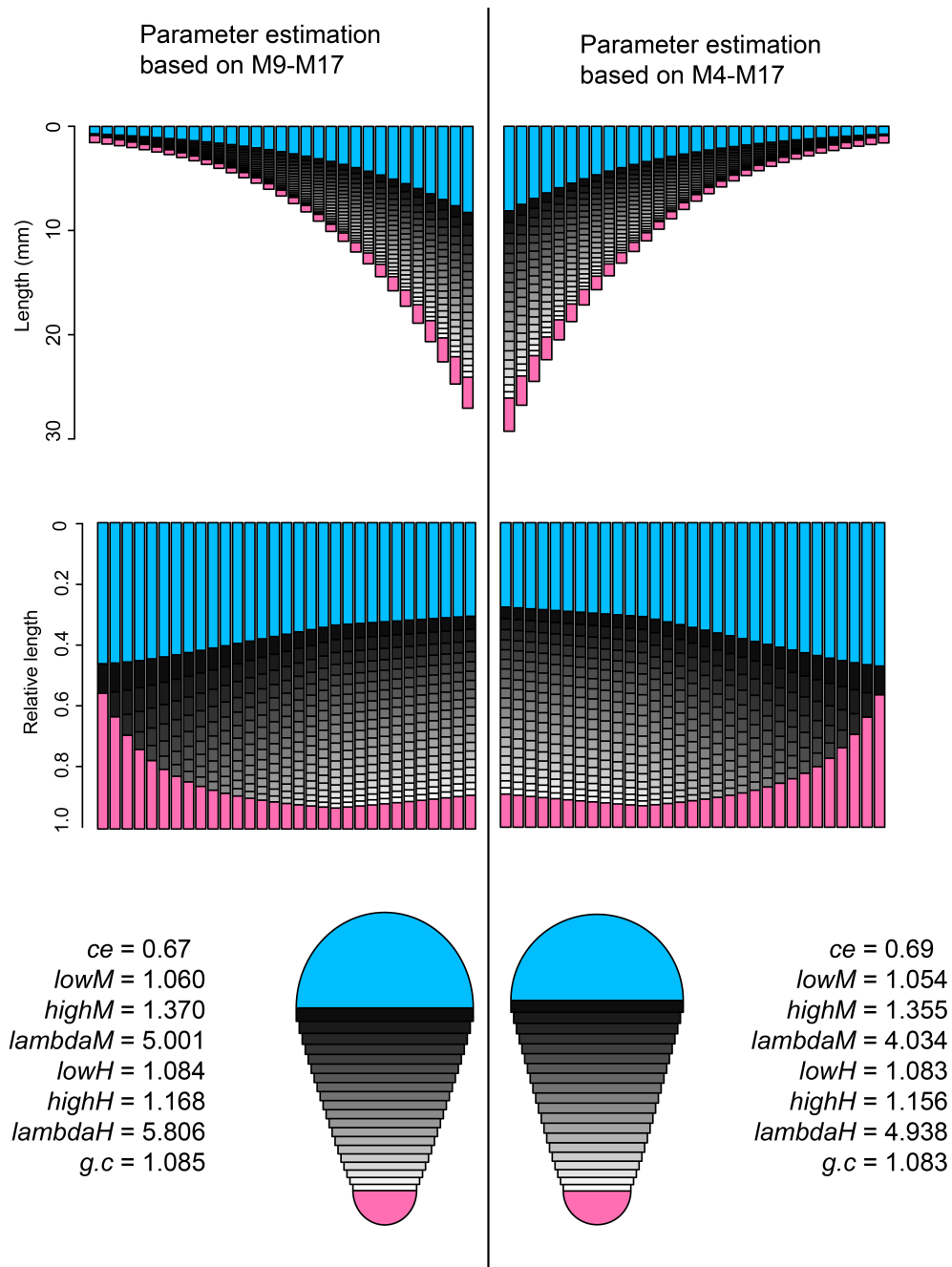


Figure S2. Parameter estimates and model output results if all meraspid specimens are used (M4-M17 instead of M9-17). This adds eleven specimens to the dataset. Parameter estimates are slightly smaller, but the curve of the growth gradient is slightly shallower (smaller values of λ). The impact on the model output is a slightly bigger trilobite at molt 31 (29.2 mm instead of 27.5 mm) with a slightly smaller cephalon relative to the trunk.

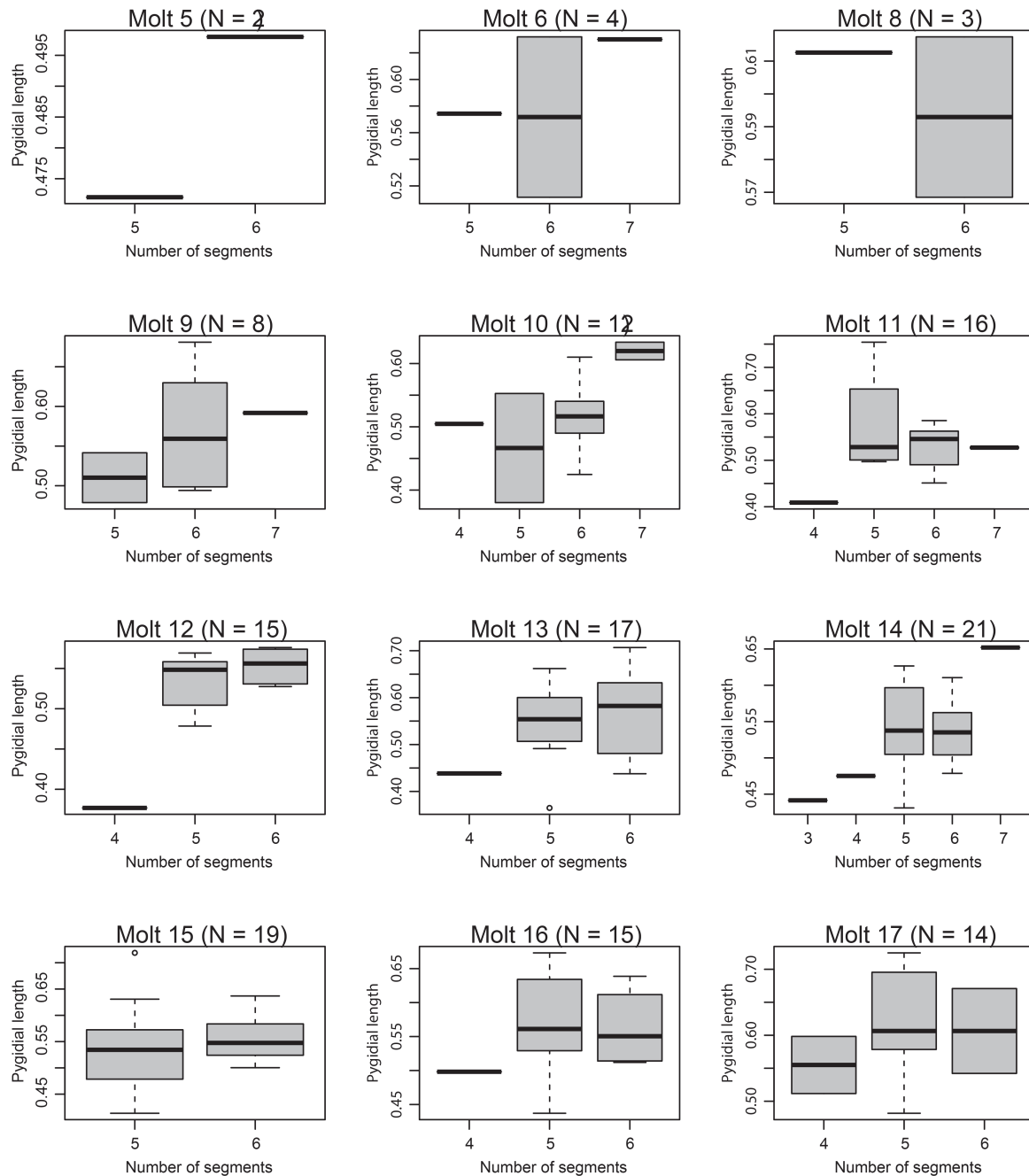


Figure S3. Boxplots showing the range of pygidial lengths for each number of segments expressed in pygidia of that molt. Not shown is one specimen with seven thoracic tergites for which pygidial length is 0.68 mm and one specimen with four thoracic tergites for which pygidial length is 0.41 mm. Likelihood tests (G-tests) do not produce any statistically significant results.